Momentum-dependent resonant inelastic X-ray scattering at the Si K edge of 3C-SiC: A theoretical study on a relation between spectra and valence band dispersion

Yunori Nisikawa*
Department of Material Science, Osaka City University, Sumiyoshi-ku, Osaka 558-8585, Japan

Muneharu Ibuki
3-2-26 Tezukayama, Nara City, Nara 631-0062, Japan

Manabu Usuda
Masago 1-4-8, Ibaraki, Osaka, 567-0851, Japan

(Dated: September 22, 2009)

We theoretically demonstrate that a resonant inelastic x-ray scattering (RIXS) with a sizable momentum transfer can be utilized to study valence band dispersion for broad band materials. We take RIXS at the Si K edge of 3C-SiC as a typical example. The RIXS spectra are calculated by systematically changing the transferred momentum, an incident photon polarization and an incident photonenergy, on the basis of an ab initio calculation. We find that the spectra depend heavily on both the transferred momentum and the incident photon polarization, and the peaks in the spectra correspond to the energies of the valence bands. We conclude that the information on the energy dispersion of valence bands can be extracted from the transferred momentum dependence of the RIXS spectra. These findings lead to further application for RIXS when investigating the band structure of broad band materials.

PACS numbers:

I. INTRODUCTION

Inelastic x-ray scattering spectroscopy is a promising method used for studying the electronic structure of matter. Since the scattering intensity in the inelastic part is much smaller than that in the elastic part, it is necessary to use x-ray optics with a high-brilliance synchrotron radiation source. It is advantageous to use a resonant enhancement by tuning the photon energy close to the absorption edge. The resonant inelastic x-ray scattering (RIXS) technique has advantages such as bulk sensitivity and element specificity. The technique can be used to investigate electronic structure in various materials.

In semiconductors such as Si and Ge, the RIXS process can be interpreted as follows. A core electron is excited to an unoccupied conduction band state of crystal momentum $\mathbf{k}_e$ by an incident photon with momentum $\mathbf{q}_1$, while a valence electron with crystal momentum $\mathbf{k}_h$ fills the core hole, emitting a photon with momentum $\mathbf{q}_2$. In the final state, electron-hole pairs remain and the momentum is conserved as $\mathbf{q}_1 - \mathbf{q}_2 = \mathbf{k}_e - \mathbf{k}_h$ in the whole process. Here, $\mathbf{q}_1 - \mathbf{q}_2$ is the transferred momentum from the photons to the electronic system. Therefore the observed RIXS spectrum contains information about the conduction and valence bands.

When the magnitude of transferred momentum $\Delta q \equiv |\mathbf{q}_1 - \mathbf{q}_2|$ is much smaller than the typical size of the crystal momentum $k_{\rm elec}$ of electrons in the solid, the momentum conservation can be written as $\mathbf{k}_e = \mathbf{k}_h$. By tuning the incident photon energy, we can indirectly select $\mathbf{k}_e$ and thereby $\mathbf{k}_h (= \mathbf{k}_e)$, depending on the dispersion of the unoccupied conduction bands. Therefore, from the excitation energy dependence of RIXS spectra,we can determine unambiguously valence band dispersion at special points, such as band edge and high symmetry point (k-selective RIXS).[1,2,3,4,5,6,7,8,9,10,11] The situation mentioned above usually corresponds to RIXS in the soft X-ray region. The k-selective RIXS in the soft X-ray region has been performed for a number of broad band materials[12,13,14,15,16,17,18,19,20] and is widely accepted as a tool for band structure investigation.[21,22,23,24,25,26,27,28,29,30,31,32]

In the case of $\Delta q \simeq k_{\rm elec}$, $\mathbf{q}_1 - \mathbf{q}_2$ can cover a wide range of the Brillouin zone and we can control its magnitude and direction by setting a scattering geometry. Therefore, we can scan $\mathbf{k}_h$ as $\mathbf{k}_h = \mathbf{k}_e - (\mathbf{q}_1 - \mathbf{q}_2)$, where we can select $\mathbf{k}_e$ by tuning the incident photon energy. We can then extract information on the dispersion of valence bands from the transferred momentum dependence of the RIXS spectra without changing the incident photon energy (k-scannable RIXS)[33]. In contrast to the k-selective RIXS experiment for broad band material, the k-scannable RIXS experiments are far from being exhaustive with the exception of experiments performed for Si,[34] Ge,[35,37] Cu[35] and NiAl[36]. In k-scannable RIXS there are two important conditions: (A)$\Delta q \gtrsim k_{\rm elec}$ (B) $\Gamma \ll W_{\rm con}$, where Γ is core level width and $W_{\rm con}$ is the bandwidth of the lowest conduction band. Condition (A) ensures the scannability while condition (B) ensures the selectivity of $\mathbf{k}_e$. These conditions also make sure the RIXS spectra is dependent on transferred momentum. (It should be mentioned that the photon energy E is required to obtain sizable momentum transfer $\Delta q \sim E/\hbar c$ but corresponding core level widths Γ are usually large.) For example, the k-scannable RIXS spectra at the K edge of Ge are nearly independent of transferred momentum.[35,37].

For RIXS at the K edge of Ge we can estimate that $\Delta q \simeq 5.6$ Å^{-1} and $k_{\rm elec} \simeq 1.1$ Å^{-1} from the K edge energy (∼11100 eV) and the lattice constant. So, the condition (A) is satisfied. In Fig.1(a) we present the band structure of Ge where the shaded bar represents the $1s$ core level width $\Gamma \simeq 2$ eV of Ge. It is clear that condition (B) is not satisfied. Therefore, the crystal momentum of the excited electron takes whole values in the first Brillouin zone, as does the momentum of the hole in the final state. Hence the RIXS spectra at the K edge does not show clear momentum dependence.

The RIXS spectra at the K edge of Si has a weak transferred momentum dependence[34], which is well reproduced by using our theoretical formulation described in Sec.II B.[38] This is because condition (A) and (B) are satisfied for RIXS at the K edge of Si: (A)$\Delta q \sim k_{\rm elec}$, where $\Delta q \simeq 0.9$ Å^{-1} and $k_{\rm elec} \simeq 1.2$ Å^{-1} are estimated from the K edge energy ($\simeq$ 1840 eV) and the lattice constant. We find (B)$\Gamma < W_{\rm con}$ from Fig. 1(b) where the band structure of Si is presented, with the shaded bar representing the $1s$ core level width $\Gamma \simeq 0.6$ eV[39,40].

Now, we consider the RIXS at the Si K edge of 3C-SiC. The band structure of 3C-SiC is presented in Fig. 1(c) with the shaded bar representing the $1s$ core level width $\Gamma \simeq 0.6$ eV. Condition (B),$\Gamma \ll W_{\rm con}$, is clearly satisfied. Condition (A) is also satisfied. Therefore, we can expect that RIXS at the Si K edge of 3C-SiC has strong transferred momentum dependence. However, to our knowledge, no k-scannable RIXS study near Si K edge of 3C-SiC has been reported, although a pioneering work on the band mapping by using k-selective RIXS at the C K edge and Si L edge has been performed.[8]

It is the purpose of this paper to demonstrate theoretically that k-scannable RIXS can be utilized to study the dispersion of valence bands for broad band materials, taking RIXS at Si K edge of 3C-SiC as a typical example. We also calculate the RIXS spectra at the C K edge of 3C-SiC and compare the experimental and theoretical spectra. This paper is organized as follows. After describing the formalism for calculation of RIXS spectra in Sec. II, we investigate transferred momentum dependence of RIXS spectra in Sec. III A. In Sec. III B and C the incident photon polarization and energy dependence of spectra are respectively presented. Sec. III D is devoted to RIXS near C K edge of 3C-SiC. Concluding remarks are presented in Section IV.

II. FORMULATION

A. Double differential scattering cross-section at K edge

RIXS at the K edge is described by a second-order process. The incident photon with energy $\hbar\omega_1$, momentum $\hbar\mathbf{q}_1$ and polarization $\mathbf{e}_1$ is virtually absorbed by exciting the $1s$ electron to the conduction band. Thena photon with energy $\hbar\omega_2$,momentum $\hbar\mathbf{q}_2$ and polarization $\mathbf{e}_2$ is emitted by filling the core-hole state with a valence electron. An independent-particle approximation seems to be appropriate, since electron correlations are expected to be weak. Using the generalized Fermi golden rule where the interaction between photons and electrons is treated by second order perturbation theory, we obtain the double differential scattering cross-section as follows;

$$\begin{aligned}\frac{d^2\sigma}{d\omega_2 d\Omega_2} \propto & \sum_{(\mathbf{k},e),(\mathbf{k}',h)} \\ & \times \frac{\left|\sum_a \exp(i\Delta\mathbf{q}\cdot\mathbf{R}_a)\overline{t_a(\mathbf{k}',h|\mathbf{e}_2)}t_a(\mathbf{k},e|\mathbf{e}_1)\right|^2}{(\epsilon_e(\mathbf{k})-\epsilon_c-\hbar\omega_1)^2+\Gamma^2/4} \\ & \times \delta^{\mathbf{G}}_{\Delta\mathbf{q},\mathbf{k}-\mathbf{k}'}\delta(\epsilon_e(\mathbf{k})-\epsilon_h(\mathbf{k}')-\hbar\omega), \end{aligned} \quad (1)$$

where $\hbar\omega = \hbar\omega_1 - \hbar\omega_2$, and $\hbar\Delta\mathbf{q} = \hbar\mathbf{q}_1 - \hbar\mathbf{q}_2$ are the energy and momentum of the final state, respectively. $\epsilon_e(\mathbf{k})$, $\epsilon_h(\mathbf{k}')$ and ϵ_c are the energy of the excited electron with crystal momentum $\mathbf{k}$ in the conduction band e, the energy of the hole with crystal momentum $\mathbf{k}'$ in the valence band h, and the energy of the core state of a specific atom (Si or C atom in this paper), respectively. The overline in the equation indicates a complex conjugate. The Γ is the $1s$ core level width of a specific atom.

The quantity

$$t_a(\mathbf{K},b|\mathbf{e}_i) \equiv \int d\mathbf{r}\overline{\psi_{\mathbf{K},b}(\mathbf{r})}\mathbf{e}_i\cdot\hat{\mathbf{p}}\phi^{1s}(\mathbf{r}-\mathbf{R}_a) \quad (2)$$

describes the transition between the bands and the $1s$ core state within the dipole approximation. $\mathbf{R}_a$ is the position vector of a specific atom in the unit cell, $\psi_{\mathbf{K},b}$ is the bloch-wave function of an electron in the band b with crystal momentum $\mathbf{K}$, and ϕ^{1s} is the $1s$-atomic orbital of a specific atom. The crystal momentum conservation for the whole process is contained in the Kronecker delta,

$$\delta^{\mathbf{G}}_{\Delta\mathbf{q},\mathbf{k}-\mathbf{k}'} \equiv \begin{cases} 0 & : \Delta\mathbf{q}-(\mathbf{k}-\mathbf{k}') \notin \mathbf{G} \\ 1 & : \Delta\mathbf{q}-(\mathbf{k}-\mathbf{k}') \in \mathbf{G} \end{cases}, \quad (3)$$

where $\mathbf{G}$ is the set of reciprocal lattice vectors.

B. Electronic structure calculation of 3C-SiC

We calculate the electronic structure using the full-potential linearized augmented-plane-wave (FLAPW) method within the local-density approximation (LDA). The local exchange-correlation functional of Vosko, Wilk and Nusair is employed.[41] The angular momentum in the spherical-wave expansion is truncated at $l_{\rm max} = 6$ and 7 for the potential and wave function, respectively. The energy cutoff of the plane wave is 12 Ry for the wave function. Figure 1(c) shows the calculated band structure of 3C-SiC. The numbers attached to bands are band indices used in this paper. From Fig. 1(c), we find that the energy of band 5 at X point is the minimum energy of

the conduction bands. The obtained band gap $E_{\rm G}^{\rm LDA}$ is 1.3 eV, which is smaller than the experimental band gap $E_{\rm G}^{\rm exp}$ ∼2.4 eV. The band gaps are often underestimated in the density-functional calculation with the LDA.

III. RESULTS AND DISCUSSION

Hereafter, we use the quantity $\hbar\xi_1 \equiv \hbar\omega_1 - (\min_{\mathbf{k}}\epsilon_5(\mathbf{k}) - \epsilon_c)$, instead of the incident photon energy $\hbar\omega_1$, to avoid problems with uncertainty in the value of the core level energy ϵ_c, treated as an input parameter in this paper. $\hbar\xi_1$ is the excited electron energy measured from the bottom of the conduction band. In addition, we plot our calculated RIXS spectra as functions of $\hbar\omega_1 - \hbar\omega_2 - \Delta\epsilon_{\rm G}$ to avoid issues with uncertainty in the value of the experimental band gap, where $\Delta\epsilon_{\rm G} = E_{\rm G}^{\rm exp} - E_{\rm G}^{\rm LDA} \simeq 1.1$ eV.

A. Transferred momentum dependence of RIXS spectra at the Si K edge

In this section, we show that the RIXS spectra strongly depend on the transferred momentum by using two kinds of configuration for the scattering. In one configuration, we can change the magnitude of transferred momentum whilst keeping its direction fixed and, in the other configuration, we can change the direction of transferred momentum, whilst keeping its magnitude fixed.

The first configuration is shown in Fig. 2(a). The magnitude of transferred momentum Δq can be changed, as $\Delta q \simeq 2|\mathbf{q}_1|\cos\theta$, by means of changing the value of θ without changing its direction (1 -1 -1). The incident photon tuned at the Si K edge excites the 1s electron to the X-point ($\hbar\xi_1 = 0.0$ eV). The corresponding hole in the final state is created according to the law of crystal momentum conservation (Eq.(3)). By changing the value of θ from 50° to 75°, the crystal momentum of the corresponding hole can be moved along the L-X line in the first Brillouin zone, as shown in Fig. 2(b), where the black circle represents the excited electron, and two dashed arrows and two white circles respectively represent the transferred momentum and the holes for $\theta = 50°$ and 75°. RIXS spectra for $\theta = 50°$, 60° and 75° are shown in Fig.3(a), where we can clearly see the strong transferred momentum dependence of RIXS spectra: two peaks around 6 and 10 eV in the spectrum for $\theta = 50°$ get close to each other and the peak around 14 eV in the spectrum moves toward lower energy, when changing θ from 50° to 75°. From Fig.3(b), we can understand the relation between the transferred momentum dependence and the valence band dispersion as follows. In Fig.3(b-1), the band dispersion along the L-X line is plotted and the black circle on the conduction band and the white circles on the valence bands respectively represent the excited electron and the holes in the final state for $\theta = 50°$ and 75°. RIXS spectra for $\theta = 50°$ and 75° are presented again in Fig.3(b-2) and (b-3), respectively. The vertical dashed and dotted lines show that the peaks in the spectra correspond to the energies of the holes. From Fig.3(b-1)-(b-3), we find that the peaks around 6, 10 and 14 eV in the spectrum for $\theta = 50°$ respectively correspond to the holes on the valence bands 4(3),2 and 1. Therefore, these peaks in the spectrum for $\theta = 50°$ move according to the valence band dispersion, which brings with it a transferred momentum dependence of RIXS spectra. In the situation mentioned above, we expect that the information on the valence band dispersion can be extracted from the transferred momentum dependence of the RIXS spectra.

We also calculate RIXS spectra using another configuration shown in Fig. 4(a). We can change the direction of the transferred momentum by means of rotating the sample around the (001)-axis by φ, without changing the magnitude of the transferred momentum $\Delta q \simeq \sqrt{2}|\mathbf{q}_1|$. It seems that this configuration lends itself more easily to experiment than the configuration shown in Fig. 2(a) because we need not change the angle between the incoming and the outgoing X-ray. The incident photon tuned at the Si K edge excites the 1s-electron to band 5 at the X-point where the energy of the conduction band is a minimum ($\hbar\xi_1 = 0.0$ eV). There are three equivalent X points (X_1, X_2 and X_3 in Fig.4(a)) in the first Brillouin zone. The wave functions of band 5 at X_1, X_2 and X_3 projected onto the p-symmetric state centering on the Si atom are respectively $P_{l=1}\psi_{\mathbf{k}=X_1,5} \propto p_x$, $P_{l=1}\psi_{\mathbf{k}=X_2,5} \propto p_y$ and $P_{l=1}\psi_{\mathbf{k}=X_3,5} \propto p_z$, as illustrated on the crystal axes in Fig. 4(a). (Here, $P_{l=1}$ is an operator of the projection onto the p-symmetric state centering on the Si atom.) Therefore, the σ-polarized incident photon tuned at the Si K edge excites the 1s electron only to the X_3-point according to the selection rule within the dipole approximation (Eq.(2)). When we change the value of φ from 45° to 90°, the crystal momentum of the hole corresponding to the electron at the X_3-point moves along the dotted arc in the first Brillouin zone as shown in Fig.4(b). The black circle in Fig.4(b) represents the excited electron, and two arrows and two white circles respectively represent the transferred momentum and the holes for $\varphi = 45°$ and 90°. The band dispersion along the dotted arc in Fig.4(b) are presented in Fig.5(a) where the white circles on bands represent the holes for $\varphi = 45°$ and 90° in the final state. The RIXS spectra for $\varphi = 45°$ and 90° are respectively presented in Fig.5(b) and (c). The vertical dashed and doted lines show that the peaks in the spectra correspond to the energies of the holes. From Fig.5(a-c), we find that the RIXS spectra depend on the direction of the transferred momentum, reflecting the valence band dispersion.

B. Incident photon polarization dependence of RIXS spectra at the Si K edge

We investigate the incident photon polarization dependence of RIXS spectra by using a configuration shown in Fig.6(a). On the crystal axes in Fig.6(a), we illustrate the wave functions of band 5 at the X-point projected onto p-symmetric states centering on the Si atom. From Fig.6(a), we find that the incident photon with π (σ)-polarization tuned at the Si K edge can excite the $1s$-electron only to the X_3 (X_2) point because of the selection rule within the dipole approximation(Eq.(2)). The corresponding hole in the final state is created at the W (Δ) point in k-space to satisfy the law of crystal momentum conservation (Eq.(3)), as shown in Fig.6(b), where the cross-section of k-space and boundaries of Brillouin zones are also presented. Therefore, the photon is emitted from the W (Δ) point in the case of the π (σ)-polarization and the energy of emitted photons with different polarization is not the same, as shown in Fig.6 (c). The spectra clearly show the strong polarization dependence. For example, the spectrum for π-polarization has one main peak at approximately 6 eV but the spectrum for σ-polarization has that at approximately 3 eV. In the above discussion, it is essential that both π and σ-polarized incident photons excite the $1s$ electron to the equivalent k-points (X_3 and X_2) but the corresponding holes are created at the non-equivalent k-points (W and Δ) because of the sizable momentum transfer in the law of crystal momentum conservation. Therefore, the strong polarization dependence is one of the characteristic features of the k-scannable RIXS which the k-selective RIXS($\Delta q \ll k_{\rm elec}$) does not have. We conclude that without changing the transferred momentum, the electronic structure at non-equivalent k-points can be investigated from the polarization dependence due to the selection rule and the law of crystal momentum conservation with a sizable momentum transfer.

C. Incident photon energy dependence of RIXS spectra near the Si K edge

In Sec. III A and B, we fixed the incident photon energy only at the Si K edge ($\hbar\xi_1 = 0.0$ eV). Here, we investigate the incident photon energy dependence of the RIXS spectra by using the configuration shown in Fig. 2 (a). The results for $\hbar\xi_1$=0.0, 2.0 and 4.0 eV are presented in Fig.7(a)-(c). The inset in each figure (a)-(c) is the band structure of 3C-SiC and the shaded bar in the inset indicates the energy of the electron excited by each incident photon from the $1s$ core level. From Fig.7(a) and (b), the momentum dependence in the spectra for $\hbar\xi_1 \simeq 0.0$ eV is also found in the spectra for $\hbar\xi_1 \simeq 2.0$ eV. This is because the $1s$ electron is excited near the X-point and has selective crystal momenta due to the deep minimum of conduction band 5 and the relatively narrow 1s core level width, as shown in the inset of Fig.7(b). Therefore, we may conclude that the features of the spectra are almost unchanged as far as the excited electron has selective crystal momenta. On the other hand, if the incident photon energy becomes larger, the crystal momentum of the excited electron can take whole values in the first Brillouin zone as does the momentum of the hole in the final state. Therefore, the peak structure of the RIXS spectra is smeared out, and the spectra have almost no dependence on the transferred momentum. This is just the case for $\hbar\xi_1 = 4.0$ eV. The spectra in Fig.7(c) have almost no dependence on the transferred momentum because the crystal momentum of the excited electron take almost whole values in the first Brillouin zone, as shown in the inset of Fig.7(c).

From the above discussion, we can predict that the spectra have transferred momentum dependence up to at least $\hbar\xi_1 = 2.0$ eV.

D. RIXS spectra near the C K edge

So far, we have concentrated on a theoretical investigation of the RIXS near the Si K edge. Last, we calculate the RIXS spectra near the C K edge of 3C-SiC by using the same formulation mentioned in Sec. II. We set the value of the $1s$ core level width of the C atom to 0.1 eV. The RIXS experiment near the C K edge of 3C-SiC, changing the incident photon energy between 283.6 eV and 295.20 eV, has been performed and the experimental RIXS spectra are presented in the Ref.[8]. In Fig.8, we compare the theoretical and experimental RIXS spectra. We calculate RIXS spectra as functions of $\hbar\omega_2 - \hbar\omega_1 + \Delta\epsilon_{\rm G}$ near the C K edge for $\hbar\xi_1 = 0.4$, 1,4, 1.9, 2,5 and 3.3 eV, these energies approximately correspond to $\hbar\omega_1$ =283.60, 284.60, 285.10, 285.70 and 286.50 eV in Fig. 1 of the Ref.[8], respectively. Each down-arrow in Fig.8 indicates the position of the origin of the experimental spectrum plotted as a function of $\hbar\omega_2 - \hbar\omega_1$. As the incident photon energy is increased from $\hbar\xi_1 = 0.4$ eV, the shapes of experimental spectra become broader and the peaks shift toward lower energy. These features can be well reproduced with our calculations. However, the position of the lowest-energy peak in each theoretical spectrum is located at slightly higher energy compared with that in each experimental spectrum. Moreover, the height of the lowest-energy peak in theoretical spectra for $\hbar\xi_1 = 2.5$ and 3.3 eV is higher than that in experimental spectra. This may be because of a linearizing procedure in the FLAPW method, which becomes less accurate for states highly deviating from the Fermi energy. Apart from detail, our formulation closely reproduces the experimental RIXS spectra near the C K edge, which supports our theoretical prediction of the RIXS at the Si K edge. Experimental investigation of RIXS at the Si K edge is highly desirable for confirmation of this.

IV. CONCLUDING REMARKS

We have investigated the resonant inelastic X-ray scattering near the Si K edge of 3C-SiC by systematically changing the transferred momenta, the incident photon polarization and the incident photon energy, on the basis of an ab initio calculation. We have demonstrated that the RIXS spectra near the Si K edge have a strong transferred momentum and incident photon polarization dependence. We have successfully reproduced the experimental RIXS spectra near the C K edge of 3C-SiC using the same formulation. From the transferred momentum dependence of RIXS spectra, we can extract information on the valence band dispersion. We can also investigate the valence band at non-equivalent k-points from the incident photon polarization dependence of the spectra.

We conclude that our results and method are not limited to the RIXS at the Si K edge of 3C-SiC. Similar results are expected in any RIXS process with a sizable momentum transfer, where the excited electron has selective crystal momenta. Therefore, we can conclude that a RIXS experiment with a sizable momentum transfer seems helpful for investigation of valence band dispersion in broad band materials, considering that RIXS is bulk-sensitive. This is in contrast to a photo emission with a lower energy photon, which is surface-sensitive.

Acknowledgments

The authors wish to thank N. Hamada for allowing them to use his FLAPW code, and A. Agui, M. Mizumaki and J. Igarashi for valuable discussion. Numerical computation was partly carried out using the Computer Facility of Yukawa Institute.

* Electronic address: nisikawa@sci.osaka-cu.ac.jp

[1] J.E. Rubensson, D. Mueller, R. Shuker, D.L. Ederer, C.H. Zhang, J. Jia, and T.A. Callcott, Phys. Rev. Lett. **64**, 1047 (1990).

[2] Y. Ma, N. Wassdahl, P. Skytt, J. Guo, J. Nordgren, P.D. Johnson, J.E. Rubensson, T. Boske, W. Eberhardt, and S.D. Kevan, Phys. Rev. Lett. **69**, 2598 (1992).

[3] K.E. Miyano, D.L. Ederer, T.A. Callcott, W.L. OBrien, J.J. Jia, L. Zhou, Q.Y. Dong, Y. Ma, J.C. Woicik, and D.R. Mueller, Phys. Rev. B **48**, 1918 (1993).

[4] J.A. Carlisle, E.L. Shirley, E.A. Hudson, L.J. Terminello, T.A. Callcott, J.J. Jia, D.L. Ederer, R.C.C. Perera, and F.J. Himpsel, Phys. Rev. Lett. **74**, 1234 (1995).

[5] C.B. Stagarescu, L.C. Duda, K.E. Smith, J.H. Guo, J. Nordgren, R. Singh, and T.D Moustakas, Phys. Rev. B **54**, R17335 (1996).

[6] J.J. Jia, T.A. Callcott, E.L. Shirley, J.A. Carlisle, L.J. Terminello, A. Asfaw, D.L. Ederer, F.J. Himpsel, and R.C.C. Perera, Phys. Rev. Lett. **76**, 4054 (1996).

[7] A. Agui, S. Shin, M. Fujisawa, Y. Tezuka, T. Ishii, Y. Muramatsu, O. Mishima, and K. Era, Phys. Rev. B **55**, 2073 (1997).

[8] J. Lüning, J.E. Rubensson, C. Ellmers, S. Eisebitt, and W. Eberhardt, Phys. Rev. B **56**, 13147 (1997).

[9] S. Eisebitt, J. Lüning, JE. Rubensson, A. Settels, PH. Dederichs, W. Eberhardt, SN. Patitsas, and T. Tiedje, J. Electron Spectrosc. Relat. Phenom. **93**,245 (1998).

[10] J. Lüning, S. Eisebitt, J.E. Rubensson, C. Ellmers, and W. Eberhardt, Phys. Rev. B **59**, 10573 (1999).

[11] A. Agui, S. Shin, and Y. Kumashiro, J. Phys. Soc. Jpn. **68**, 166 (1999).

[12] L. Lin, G.T. Woods, and T.A. Callcott, Phys. Rev. B **63**, 235107 (2001).

[13] J.D. Denlinger, J.A. Clack, J.W. Allen, G.H. Gweon, D.M. Poirier, C.G. Olson, J.L. Sarrao, A.D. Bianchi, and Z. Fisk, Phys. Rev. Lett. **89**, 157601 (2002).

[14] AV. Sokolov, EZ. Kurmaev, J. MacNaughton, A. Moewes, NA. Skorikov, and LD. Finkelstein, JETP Lett. **77**, 108 (2003).

[15] AV. Sokolov, EZ. Kurmaev, S. Leitch, A. Moewes, J. Kortus, LD. Finkelstein, NA. Skorikov, C. Xiao, and A. Hirose, J. Phys.: Condens. Matter **15**, 2081 (2003).

[16] PF. Karimov, NA. Skorikov, EZ. Kurmaev, LD. Finkelstein, S. Leitch, J. MacNaughton, A. Moewes, and T. Mori, J. Phys.: Condens. Matter **16**, 5137 (2004).

[17] VN. Strocov, T. Schmitt, JE. Rubensson, P. Blaha, T. Paskova, and PO. Nilsson, Phys. Status Soldi B **241**, R27 (2004).

[18] V.N. Strocov, T. Schmitt, J.E. Rubensson, P. Blaha, T. Paskova, and P.O. Nilsson, Phys. Rev. B **72**, 085221 (2005).

[19] D. Eich, O. Fuchs, U. Groh, L. Weinhardt, R. Fink, E. Umbach, C. Heske, A. Fleszar, W. Hanke, E.K.U. Gross, C. Bostedt, T.v.Buuren, N. Franco, L.J. Terminello, M. Keim, G. Reuscher, H. Lugauer, and A. Waag, Phys. Rev. B **73**, 115212 (2006).

[20] L. Weinhardt, O. Fuchs, E. Umbach, C. Heske, A. Fleszar, W. Hanke,and J.D.Denlinger, Phys. Rev. B **75**, 165207 (2007).

[21] PD. Johnson, and YJ. Ma, Phys. Rev. B **49**, 5024 (1994).

[22] M. vanVeenendaal, and P. Carra, Phys. Rev. Lett. **78**, 2839 (1997).

[23] J.A. Carlisle, E.L. Shirley, L.J. Terminello, J.J. Jia, T.A. Callcott, D.L. Ederer, R.C.C. Perera, and F.J. Himpsel, Phys. Rev. B **59**, 7433 (1999).

[24] EL. Shirley EL, J. Electron Spectrosc. Relat. Phenom. **110**, 305 (2000).

[25] JA. Carlisle, SR. Blankenship, LJ. Terminello, JJ. Jia, TA. Callcott, DL. Ederer, RCC. Perera, and FJ. Himpsel, J. Electron Spectrosc. Relat. Phenom. **110**, 323 (2000).

[26] AV. Sokolov, LD. Finkelstein, EZ. Kurmaev, S. Shin, R. Karimov, NA. Skorikov, and AV. Postnikov, J. Electron Spectrosc. Relat. Phenom. **137**, 591 (2004).

[27] F. Gel'mukhanov, and H. Ågren, Phys. Rep. **312**, 91 (1999).

[28] S. Eisebitt, J. Lüning, JE. Rubensson, and W. Eberhardt, Phys. Status Soldi B **215**, 803 (1999).

[29] S. Eisebitt, and W. Eberhardt, J. Electron Spectrosc. Relat. Phenom. **110**, 335 (2000).

[30] A. Kotani, and S. Shin, Rev. Mod. Phys. **73**, 203 (2001).

[31] T. Ruf, Applied Phys. A **76**, 21 (2003).
[32] EZ. Kurmaev, Inorg. Mater. **41**, S1 (2005).
[33] Y. Ma, Phys. Rev. B **49**, 5799 (1994).
[34] Y. Ma, K. E. Miyano, P. L. Cowan, Y. Aglitzkiy, and B. A. Karlin, Phys. Rev. Lett. **74**, 478 (1995).
[35] A. Kaprolat and W. Schülke, Applied Phys. A **65**, 169 (1997).
[36] H. Enkisch, A. Kaprolat, W. Schulke, M.H. Krisch, and M. Lorenzen, Phys. Rev. B **60**, 8624 (1999).
[37] Y. Nisikawa, M. Usuda, J. Igarashi, H. Shoji, and T. Iwazumi, J. Phys. Soc. Jpn. **73**, 970 (2004).
[38] Y. Nisikawa, M. Usuda, and J. Igarashi, J. Phys. Soc. Jpn. **73**, 3171 (2004).
[39] J. H. Scofield, Phys. Rev. **179**, 9 (1969).
[40] V. O. Kostroun, M. H. Chen, and B. Crasemann, Phys. Rev. A **3**, 533 (1971).
[41] S. H. Vosko, L. Wilk, and M. Nusair, Can. J. Phys. **58** 1200 (1980).
[42] S. Logothetidis, HM. Polatoglou, J. Petalas, D. Fuchs, and RL. Johnson, Physica B **185**, 389 (1993).
[43] B. Wenzien, P. Kackell, F. Bechstedt, and G. Cappellini, Phys. Rev. B **52**, 10897 (1995).

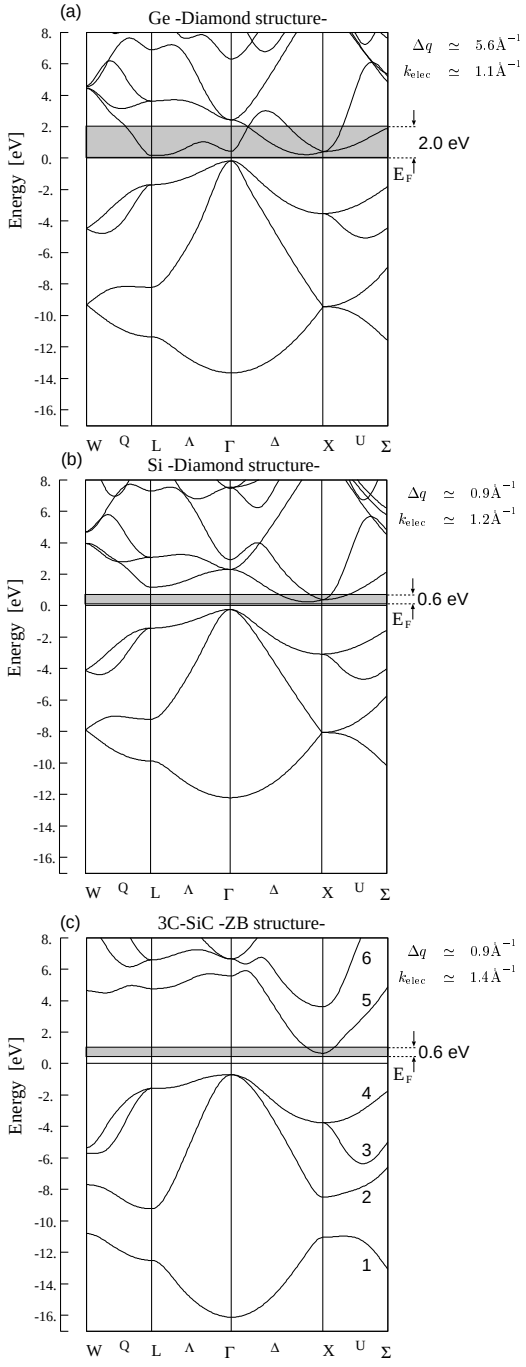

FIG. 1: The band structure of (a)Ge, (b)Si, and (c)3C-SiC calculated using density-functional theory (The details about the calculation method are described in Sec.II B). The shaded bars respectively represent the $1s$ core level widths of Ge (a) and Si (b,c) atoms. The numbers attached to the band lines in figure (c) are the band indices.

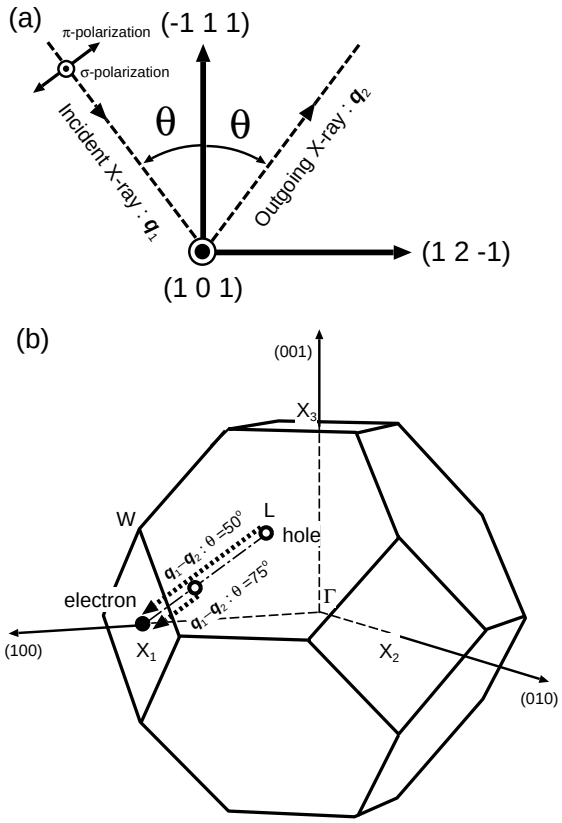

FIG. 2: (a) The configuration for RIXS. The geometrical relation between the crystal axes of 3C-SiC and the momentum of the incident and outgoing X-ray are presented. (b) The crystal-momenta of an electron-hole pair in the final state are presented in the first Brillouin zone. The dashed arrows represent the transferred momentum for $\theta = 50^\circ$ and 75°.

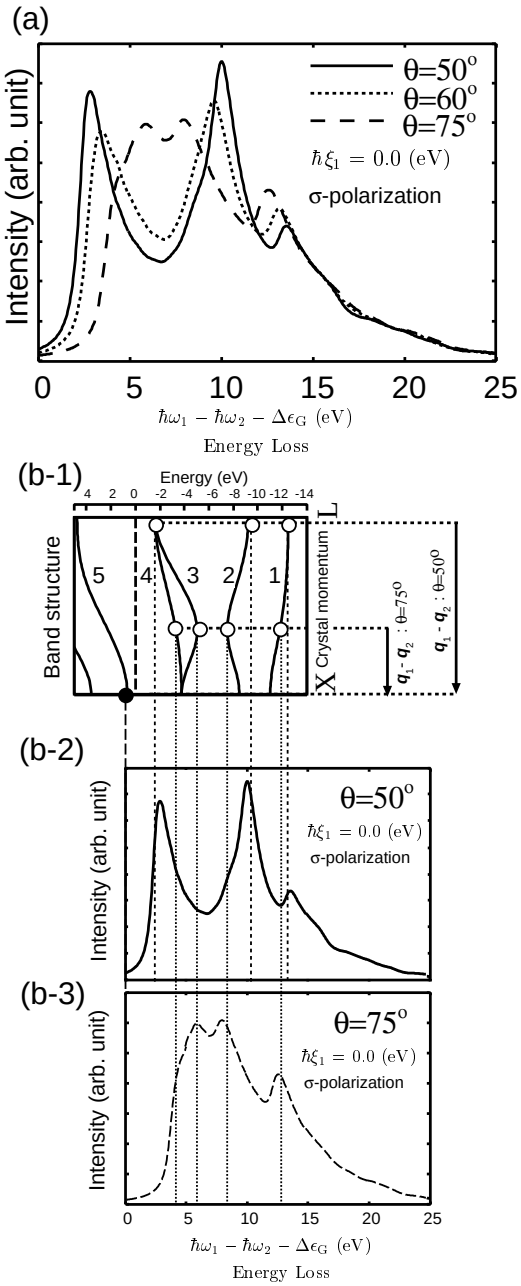

FIG. 3: (a) The transferred momentum dependence of RIXS spectra. (b) The relation between the transferred momentum dependence of RIXS spectra and the valence band dispersion. The vertical dotted and dashed lines are guides for the eye: (b-1) The band dispersion along the L-X line. The black circle on the conduction band and the white circles on the valence bands respectively represent the excited electron and the hole in the final state for $\theta = 50^\circ$ and 75°. RIXS spectra for $\theta = 50^\circ$ (b-2) and 75°(b-3).

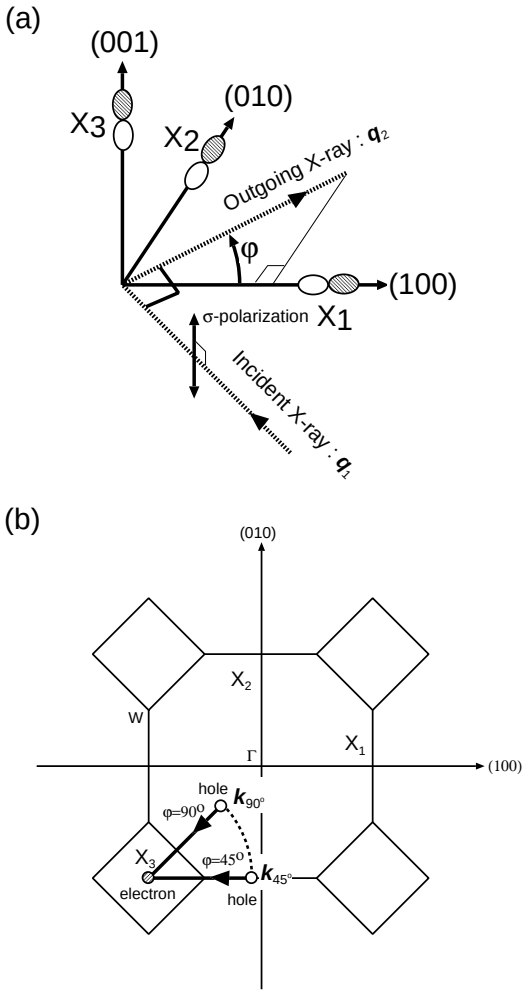

FIG. 4: (a) The configuration for RIXS, where the angle between the incident and outgoing momentum is fixed to 90°. The geometrical relation between the crystal axes of 3C-SiC and the momentum of incident and outgoing X-ray are presented. The wave functions of conduction-band 5 at X-point, projected onto p-symmetric states centering on the Si atom are illustrated on the crystal axes. (b) The crystal-momenta of the electron-hole pair in the final state are presented in the cross-section of the Brillouin zone. The arrows indicate the transferred momenta for $\varphi = 45^\circ$ and 90°.

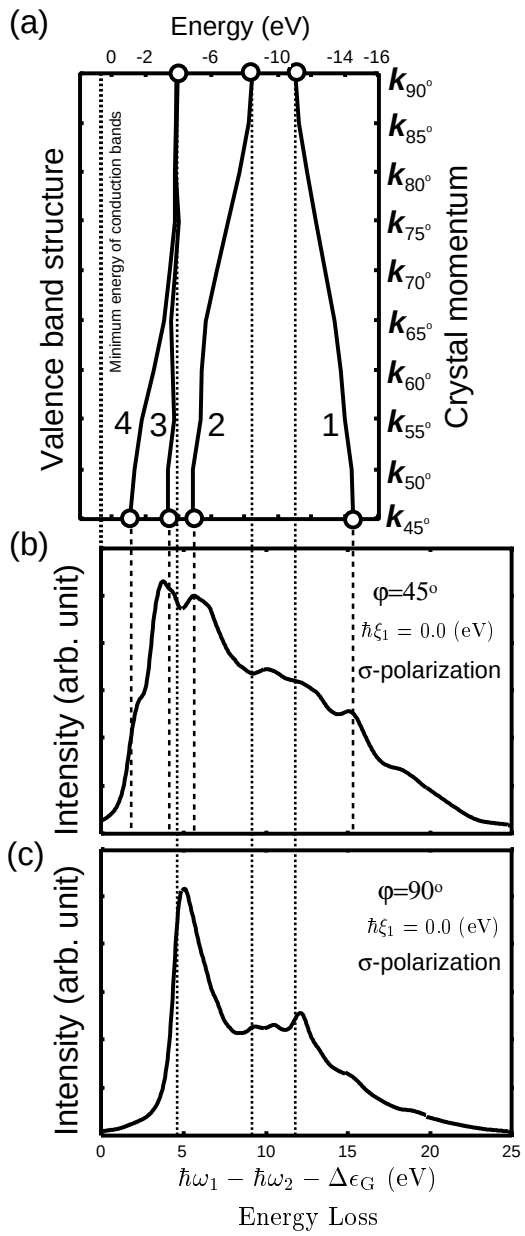

FIG. 5: The relation between valence band dispersion and spectra. The dotted and dashed lines are guides for the eye: (a) The valence band dispersion along the dotted arc in Fig.4. The white circles on the band lines represent the valence band holes for $\varphi = 45°$ and $90°$ in the final state. (b). RIXS spectra for $\varphi = 45°$(b) and $90°$(c).

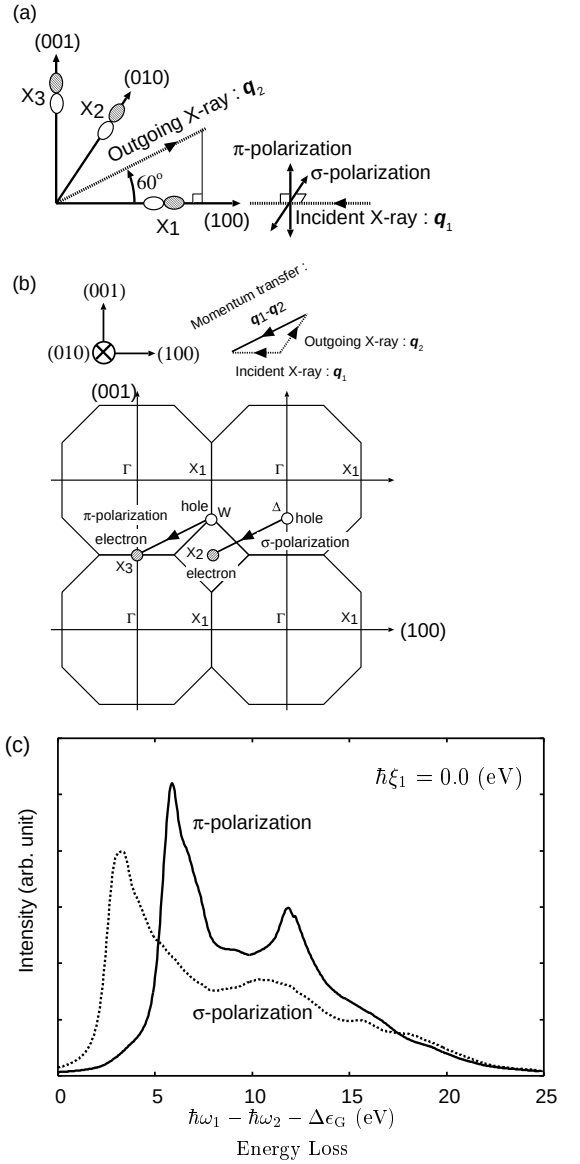

FIG. 6: (a) The configuration for the RIXS to investigate the dependence of the incident photon polarization. The geometrical relation between crystal axes of 3C-SiC and the momentum of the incident and outgoing X-ray are presented. The wave functions of conduction band 5 at the X_1, X_2 and X_3-point, projected onto p-symmetric states centering on the Si atom are illustrated on the crystal axes. (b)For π and σ-polarization, the crystal-momenta of the electron-hole pair in the final state are presented in the cross-section of k-space. The boundaries of the Brillouin zone are also presented. The arrows indicate the transferred momenta. (c) The incident photon polarization dependence of RIXS spectra.

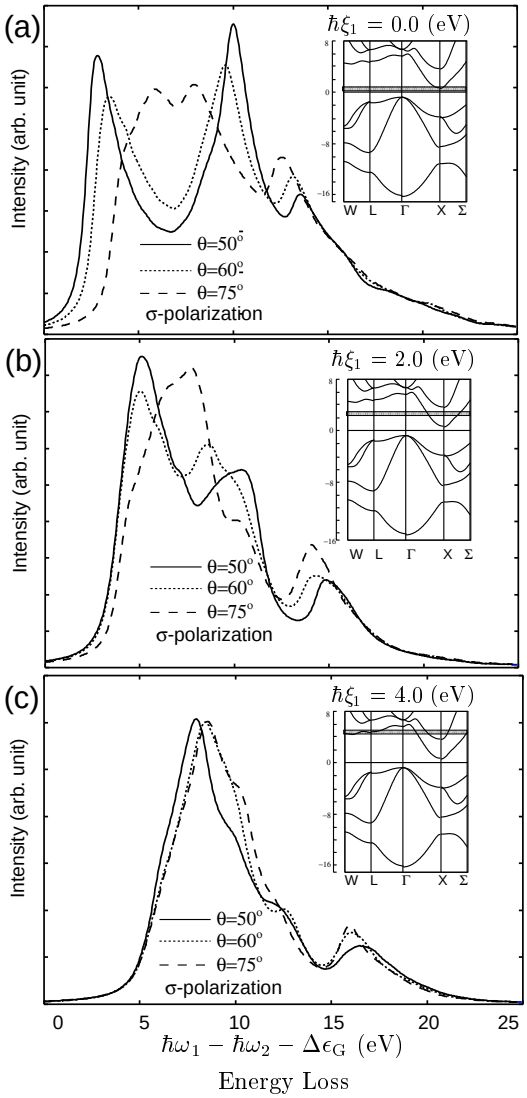

FIG. 7: Theincident photon energy dependence of RIXS spectra near the Si K edge for $\theta = 50°$, $60°$ and $75°$: $\hbar\xi_1$ = (a)0.0, (b)2.0 and (c)4.0 eV. (Inset) The energy of the excited electron is indicated by the shaded bar in the band structure of 3C-SiC .

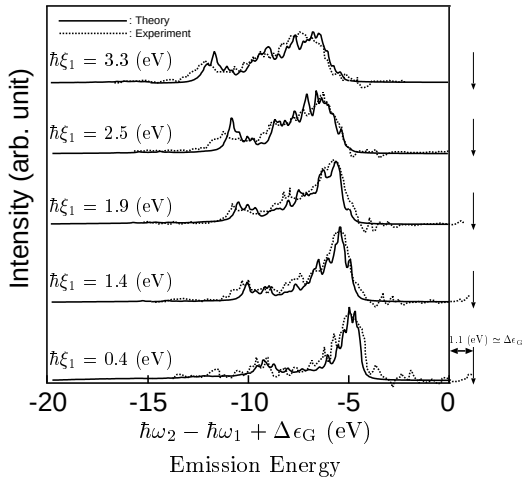

FIG. 8: The comparison between the theoretical (solid lines) and experimental(dotted lines) RIXS spectra near the C K edge. $\hbar\xi_1$ =0.4, 1,4, 1.9, 2,5 and 3.3 eV, approximately correspond to $\hbar\omega_1$ =283.60, 284.60, 285.10, 285.70 and 286.50 eV in Fig. 1 of the Ref.[8], respectively. Each down-arrow indicates the position of the origin of the experimental spectrum plotted as a function of $\hbar\omega_2 - \hbar\omega_1$.